

Episodic riverine influence on surface DIC in the coastal Gulf of Maine

Joseph Salisbury^{a,*}, Douglas Vandemark^a, Christopher Hunt^a, Janet Campbell^a, Bror Jonsson^b, Amala Mahadevan^b, Wade McGillis^c, Huijie Xue^d

^a Institute for the Study of Earth, Oceans and Space, University of New Hampshire, Durham, NH 03825, USA

^b Department of Earth Sciences, Boston University, Boston, MA 02215, USA

^c Lamont–Doherty Earth Observatory, Columbia University, Palisades, NY 10964, USA

^d School of Marine Science, University of Maine, Orono, ME 04469, USA

ARTICLE INFO

Article history:

Received 9 September 2008

Accepted 23 December 2008

Available online 3 January 2009

Keywords:

Coastal

Dissolved inorganic carbon

CO₂, Air–sea exchange Land–Ocean

ABSTRACT

Anomalously high precipitation and river discharge during the spring of 2005 caused considerable freshening and depletion of dissolved inorganic carbon (DIC) in surface waters along the coastal Gulf of Maine. Surface pCO₂ and total alkalinity (TA) were monitored by repeated underway sampling of a cross-shelf transect in the western Gulf of Maine (GOM) during 2004–05 to examine how riverine fluxes, mixing, and subsequent biological activity exert control on surface DIC in this region. Most of the variability in surface DIC concentration was attributable to mixing of low DIC river water with higher DIC, saline GOM waters, but net biological uptake of DIC was significant especially during the spring and summer seasons. The extent and persistence of the coastal freshwater intrusion exerted considerable influence on net carbon dynamics. Integrated over the 10-m surface layer of our study region ($\sim 5 \times 10^4$ km²), net biological DIC uptake was 0.48×10^8 mol C during April–July of 2004 compared to 1.33×10^8 mol C during April–July of 2005. We found the temporal signature and magnitude of DIC cycling to be different in adjacent plume-influenced and non-plume regions. Extreme events such as the freshwater anomaly observed in 2005 will affect mean estimates of coastal carbon fluxes, thus budgets based on short time series of observations may be skewed and should be viewed with caution.

© 2008 Elsevier Ltd. All rights reserved.

1. Introduction

The coastal ocean acts as a medium of exchange for oceanic, atmospheric and terrestrial carbon pools. Its function in mediating processes of air–sea carbon flux, DIC sequestration and export, are subjects of increasing inquiry as the community seeks to constrain global carbon budgets. From a modeling perspective, an understanding of the modulation of the coastal DIC pool via biological processes remains particularly enigmatic (Mahadevan and Campbell, 2002). Land-to-ocean fluxes of freshwater and associated constituents confound the issue by providing inputs of inorganic nutrients and buoyancy capable of stimulating and maintaining productivity, while providing labile organic matter that can fuel heterotrophy. This is reflected in the ongoing debate in which numerous studies of coastal carbon dynamics have failed to conclude whether the coastal ocean is a net source or sink of atmospheric carbon. Several authors have shown that coastal systems are net sources of CO₂ to the atmosphere (Cai and Wang,

1998; Frankignoulle et al., 1998; Borges and Frankignoulle, 2002). In contrast, studies focusing on shelf regions, particularly those affected by large rivers, suggest that coastal systems can sequester globally significant amounts of atmospheric carbon dioxide on annual time scales (Tsunogai et al., 1999; Liu et al., 2000; Cai, 2003; Kortzinger, 2003). Recent global assessments of coastal carbon fluxes represent ambitious attempts to scale up limited coastal data sets (Borges, 2005; Borges et al., 2005; Cai et al., 2006). However, the authors of these assessments concede that limitations in both the temporal and spatial density of data hamper efforts to adequately capture the carbon variability inherent in these complex coastal systems.

The degree to which extreme environmental conditions such as hurricanes and anomalously high discharge affect mean coastal carbon budgets has not been widely studied. However, such events are known to elicit physical and biological responses that induce rapid transformations in the carbon pools and large transfers between terrestrial, oceanic and atmospheric reservoirs. For example, mixing that occurs during high winds can rapidly ventilate already supersaturated waters causing an increase in sea–air exchange of gases. Hurricanes have been reported to ventilate the surface oceans significantly in the sub-tropical North Pacific

* Corresponding author.

E-mail address: joe.salisbury@unh.edu (J. Salisbury).

(Kawahata et al., 2001), the sub-tropical North Atlantic (Bates et al., 1998) the North Atlantic (Perrie et al., 2004), and in the Caribbean (Wanninkhof et al., 2007). In the sub-arctic North Pacific, the occurrence of storms was shown to influence net CO₂ dynamics via coupled biological–physical processes that include nutrient injection, light limitation and increased air–sea exchange of CO₂ (Fujii and Yamanaka, 2008). High runoff events have also been cited as having a dramatic effect on terrestrial fluxes into coastal waters. Depetris and Kempe (1993) found that the transport of total organic carbon (TOC) doubled (from 4.43 to 8.43 Tg yr⁻¹) as a result of major El Niño Southern Oscillation-induced flooding of the Parana River. Avery et al. (2004) reported that between one-third and one-half of the annual river flux of dissolved organic carbon (DOC) to Long Bay in the southeastern US occurred as a result of hurricanes. Yuan et al. (2004) estimated that the Mississippi's plume, augmented by the passing of Hurricane Lili and Tropical Storm Barry in 2001, may have transported 0.54 Tg of DOC over a 2-week period. This represents approximately one-fourth of the watershed's average annual DOC flux into the Gulf of Mexico.

In this paper we examine the comparative dynamics of surface DIC along a cross-shelf transect in the Gulf of Maine during 2004 and 2005 and document the effects of freshwater mixing and biology on DIC distributions. We then focus on changes in the biologically mediated DIC (DIC_{bio}) pool, comparing differences in DIC cycling in two different coastal salinity regions to identify the effects of riverine discharge. The presence of an expansive low-salinity surface layer due to anomalous high runoff during April–July 2005 was associated with a more intense biological drawdown of DIC compared to the same time period in 2004.

2. Site and methods

The Gulf of Maine (GOM) is a unique, productive continental shelf sea bounded by Cape Cod to the south and Nova Scotia to the northeast (Fig. 1). The entire Gulf is macro-tidal, with the highest tides on earth found in its easternmost reach, the Minas Basin. A key circulation feature in the GOM is the Maine Coastal

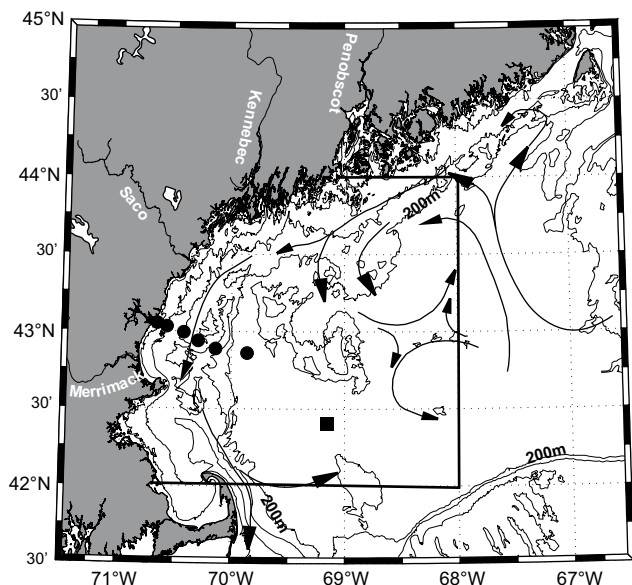


Fig. 1. Gulf of Maine, area of interest, cruise track and stations. The Western Gulf of Maine. The main area of interest is enclosed by the box which contains 49,805 km² of ocean surface. Monthly (ca) cruise track proceeds along Coastal Observation and Analysis (COOA) station coordinates (dots). Virtual offshore endmember station (square). A generalized circulation pattern in the Gulf of Maine is shown with arrows.

Current (MCC) whose counterclockwise flow typically delivers freshwater and constituents from the rivers northeast to our study region (Townsend et al. in Robinson and Brink, 2005). The Kennebec–Androscoggin River System (henceforth referred to as the Kennebec) is the largest river system entering the area of interest and is its predominate source of local discharge. However during upwelling-favorable winds, discharge from the Merrimack River (Fig. 1) can spread over the region and contribute significant freshwater (Fong et al., 1997). There is a strong seasonal signal in salinity and along-shore velocity of the MCC caused by the freshwater inputs of the rivers entering the western GOM. Surface salinity within the coastal current during the spring freshet is typically 2 psu below ambient, and along-shore currents in the surface layer are directed southwestward at speeds of 0.10–0.50 m s⁻¹. The thickness of the plume is variable, but is generally 10–20 m over water depths of 50–150 m (Geyer et al., 2004), the approximate depth range occupied by the plume (Fig. 1). The along-coast freshwater transport within the region of coastal influence varies considerably due to variations in wind stress, but on time scales of weeks to months it follows the variations of riverine input with a time lag that is consistent with the advective velocity (Geyer et al., 2004). Precipitation and discharge regimes during the April–June (2004–2005) sampling periods were not typical. Based on USGS discharge data (USGS), combined discharge of the Merrimack, Saco and Kennebec Rivers were approximately 7% and 70% above the 20-year mean during April–June 2004 and 2005, respectively. Precipitation over the Gulf of Maine Watershed reflects this trend with an average precipitation anomaly of +9% during April–June 2004 and +78% during April–June 2005, based on a NOAA National Climatic Data Center 25-year mean (Michael Rawlins, personal communication).

Beginning in April 2004, we have conducted cruises at approximately monthly intervals. The cruises embark from Portsmouth, NH, cross over the Jeffrey's Ledge fishing grounds and continue to Wilkinson Basin, one of 3 deep-water basins in the Gulf of Maine (Fig. 1). This transect bisects the western half of the ~50,000 km² study region in the Western Gulf of Maine (Fig. 1). Our surveys are sponsored by the University of New Hampshire's (UNH) National Oceanic and Atmospheric Administration (NOAA) Coastal Ocean Observation and Analysis Center (COOA). Cruises took place aboard the UNH Gulf Challenger on 18 dates between 4/19/04 and 12/17/05. Discrete surface samples for TA and pH were taken at each station (Fig. 1) with Niskin bottles at 1-m depth according to DOE protocols (DOE, 1994), and were analyzed within two weeks. TA was analyzed by end-point titration at constant ambient temperature with 0.1 N HCl to pH 4.5 using an automated titrator (Radiometer ION 570; precision ±3.2 μmol kg⁻¹). The mean of three determinations is used. Certified reference materials (CRMs) were used to ensure the precision of the TA determinations (Dickson, 2001). pH was measured from the same sample using a combination electrode (Radiometer ION 570) using a 3-point calibration of Thermo-Orion NIST traceable pH buffers. The precision of the pH measurement (±0.007 unit) was estimated from periodic determinations of newly opened CRM. Estimates of precision do not include the effects of sample storage or gas exchange, which are assumed to be minimal.

Water was pumped continuously from ~1.5 m depth at a rate of 3.5 L min⁻¹ to shipboard flow-through systems that measured at a frequency of 1 s⁻¹. Continuous measurements of salinity and sea surface temperature (SST) were made using a Seabird (SBE 45) instrument. To measure pCO₂, intake water from the system was split to a three-chamber equilibrator, similar to that described by Wanninkhof and Thoning (1993). Sample air was dried with a Naphion® drying system and pumped to a non-dispersive

infrared gas analyzer (Li-cor[®], Li-6262). The gas analyzer was calibrated twice-daily using ultra-pure nitrogen and two gas mixtures with CO₂ molar fraction of 340 and 812 ppm (Scott-Marrin[®]). Corrections of the data for water vapor pressure and sea surface temperature were carried out according to DOE protocols (1994). Flow-through data, which were always taken during daylight hours, were sub-sampled at 20 s. Atmospheric pCO₂ was periodically measured underway by drawing ambient air from the ship's bow through a length of Teflon tube directly into the gas analyzer. Atmospheric pCO₂ in dried air was converted to moist air values using the methods of DOE (1994). Precision of pCO₂ measurements is estimated to be $\sim \pm 3 \mu\text{atm}$. TA was estimated along each cruise track using empirical salinity–TA relationships. Although a robust linear relationship between salinity and TA was found for the entire transect dataset ($n = 224$, $r^2 = 0.97$, RMSE = 11), we chose to fit a more precise TA–salinity curve for each cruise (linear or 2-degree polynomial, Table 1) in order to capture finer-scale TA variability caused by processes such as calcite production and dissolution, phytoplankton production, and respiration (average cruise TA RMSE = 6.0). We note that the zero intercept of the entire salinity–TA regression was $358 \mu\text{mol kg}^{-1}$, which is consistent with the mean of all samples from the UNH database taken in the Kennebec River at 0 psu ($352 \mu\text{mol kg}^{-1}$, $n = 27$).

In addition to the sampled along-transect data, we used the salinity fields from a continually run, operational ocean circulation model (OCM) of the Gulf of Maine (Xue et al., 2005) to estimate the spatial distribution of the river influence. This model is run and maintained at the University of Maine, with realistic winds, river discharge, heat and freshwater fluxes, and boundary conditions from a larger circulation model. The temperature, salinity and velocity fields, saved at 3-h intervals, have been rigorously tested against available observations (Xue et al., 2005). The extent of riverine influence was estimated by comparing model salinity (S) in each grid cell, against the mean model salinity S_{mean} , for the entire Gulf of Maine. A simpler approach using a fixed salinity value as a threshold to differentiate between riverine and oceanic dominance was tried, but rejected due to the large seasonal and inter-annual variability of allochthonous freshwater entering from outside the Gulf of Maine (Petrie, 2007). Instead, we calculated the “effective freshwater height, H_{FW} ” as the height of freshwater needed to lower the salinity from S_{mean} to the modeled value S in each column of grid cells, where the depth of water/column height is H , i.e. $H_{\text{FW}} = H(S - S_{\text{mean}})/S_{\text{mean}}$. H_{FW} , calculated in this way and shown in Fig. 2, evolves in space and time and is thought to provide

a more effective estimate of the extent of local riverine influence on the coastal ocean than surface salinity alone. However we note that our methods will produce a slight underestimate of the extent of riverine influence, as both the much smaller plume regions are included with the offshore regions in the estimate of S_{mean} . Since S_{mean} is a time-dependent mean, salinity modulations in the entire Gulf of Maine resulting from changes in offshore salinity can offset or intensify the riverine signal. For example, the extent of riverine influence estimated from HFW during September–November 2005 is lower than in April–May 2005 even though both periods have similar discharge, because S_{mean} was lower in April–May 2005. Indeed the position and spatial extent of riverine influence is not necessarily correlated with discharge and is probably more strongly affected by wind-induced and residual tidal currents (Fong and Geyer, 2002).

DIC was estimated using measured pCO₂, temperature, salinity and estimated TA as inputs into the carbonate equilibrium equations given in CO2SYS (Lewis and Wallace, 1998) with pK values and alkalinity constants as reported in Cai and Wang (1998). More recently published pK values were tested (Millero et al., 2006), but the difference in the resultant DIC estimates was insignificant at the salinities we encountered (~ 27 – 32). The estimation of DIC using pCO₂ and estimated TA, henceforth referred to as observed DIC (DIC_{observed}), has an average estimated error of $\pm 7 \mu\text{mol kg}^{-1}$. Variability in the DIC_{observed} field is the in-situ concentration of DIC arising from perturbations of air-sea exchange, biological activity, calcite dynamics and mixing of the landward endmember into the ocean.

The air-sea CO₂ flux (F_{CO_2}) was estimated using

$$F_{\text{CO}_2} \left(\text{mol C m}^{-2} \text{ d}^{-1} \right) = k S_{\text{m}} (\text{pCO}_{2\text{sw}} - \text{pCO}_{2\text{atm}}) \quad (1)$$

where k is the gas transfer (or piston) velocity, S_{m} is the dissolved gas solubility in seawater as function of salinity and temperature, and the difference term is between the partial pressures of carbon dioxide in the surficial air and sea boundary layers. The gas transfer velocity parameterization is from Wanninkhof (1992). Our implementation of (F_{CO_2}) utilizes the hourly wind option in the k algorithm and hourly wind measurements obtained from NDBC station IOSN3 located centrally within this study region where these wind estimates are interpolated in time onto each shipboard seawater estimate (20 s sample rate) of pCO₂, salinity, and temperature. We do not use our single day shipboard pCO_{2atm} data to extrapolate to a monthly mean atmospheric estimate for the air-sea flux. Instead, we use a monthly average for the free troposphere northern hemisphere atmospheric pCO_{2atm} obtained from NOAA's Mauna Loa continuous observing station. This choice is made because sporadic estimates of observed local episodic daily variability of ~ 10 – $20 \mu\text{atm}$ in atmospheric levels, arising due to air advected from the continent, would lead to large uncertainty in a monthly estimate (cf. Padin et al., 2007). It is also made because this NOAA data record represents a readily accessible continuous tropospheric dataset for our study period. This assumption that a Mauna Loa monthly mean lies near the regionally-observed mean value has been checked using the hourly CO₂ buoy atmospheric data and a data-informed free tropospheric model estimate at a latitude of 44 deg. N (pers. communication, P. Tans). We find that discrepancies are less than 3–5 μatm in any month of the year and of negligible impact on this study.

For each cruise biologically mediated DIC (DIC_{bio}) was estimated as the difference between a curve assumed to mix conservatively with salinity (DIC_{mix}), and the sum of DIC_{observed}, plus the daily mass of DIC added or removed by air-sea exchange (Fig. 3a, Table 2). This method of analysis provides additional detail over SST normalizations used to remove the thermal modulation of in-water

Table 1
Equations used to estimate TA for each cruise.

Cruise date	TA equation ($x = \text{salinity}$)
4/22/04	$59.5x + 270$
5/21/04	$-0.14x^2 + 61.7x + 348$
6/16/04	$56.1x + 377$
6/17/04	$56.3x + 361$
7/21/04	$-0.6x^2 + 75.1x + 392$
8/16/04	$-0.7x^2 + 77.0x + 382$
10/29/04	$55.8x + 388$
12/6/04	$55.2x + 414$
1/30/05	$57.9x + 328$
3/18/05	$-0.5x^2 + 73.9x + 353$
4/6/05	$-0.7x^2 + 83.3x + 271$
5/10/05	$-0.3x^2 + 68.4x + 247$
6/17/05	$59.9x + 255$
7/12/05	$55.8x + 370$
8/16/05	$-0.7x^2 + 32.3x + 349$
9/13/05	$55.5x + 397$
10/21/05	$55.2x + 401$
12/19/05	$55.0x + 408$

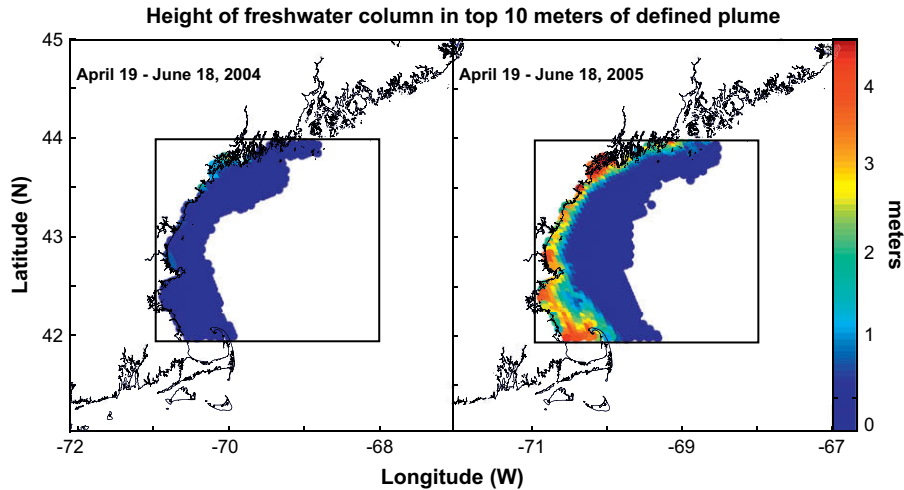


Fig. 2. Comparing the average height of freshwater column in the top 10 m, April 20–June 19, 2004 and 2005. The OCM was used to estimate freshwater column height (see text). The colored area signifies the plume region, which has the threshold of at least 5 cm freshwater in the surface 10 m. The figure shows the average height for April 19–June 18, 2004 (a) and 2005 (b). Based on an 80-year USGS record, the spring of 2005 was among the wettest on record for the drainage basins discharging into the region of interest. (For interpretation of the references to color in this figure legend, the reader is referred to the web version of this article.)

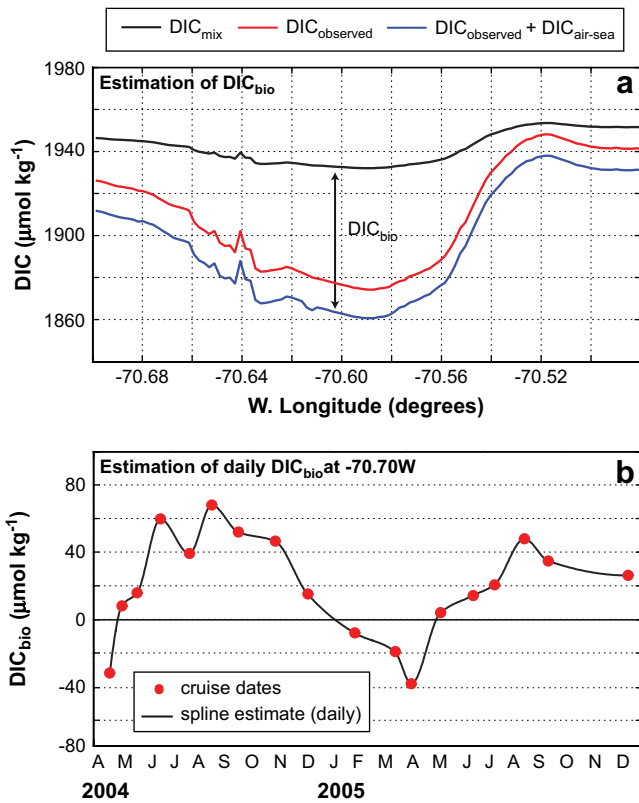


Fig. 3. Estimated DIC products. DIC parameters used in the paper estimated using a combination of discrete determinations and continuous flow-through measurements. (a) DIC_{bio} estimated as the difference between a DIC curve assumed to mix conservatively with salinity (DIC_{mix}) and the sum of observed DIC plus the daily mass of DIC added or removed by air-sea exchange $DIC_{bio} = DIC_{mix} - (DIC_{observed} + DIC_{air-sea})$. The $DIC_{air-sea}$ is the estimated daily mass of DIC exchanged from the top 10 m (i.e. $DIC_{air-sea} = \text{air-sea flux} \times 10 \text{ m/water depth}$). DIC mixing anomaly (DIC_{mix}) is produced by mixing fresh and oceanic DIC endmembers across the salinity gradient. (b) Daily DIC_{bio} estimate using piecewise cubic hermite interpolating polynomial spline (pchip, Matlab™). A daily time step was employed across the (ca) monthly data at longitudinal intervals of 0.01 degrees (Fig. 2c).

CO_2 (e.g. Takahashi et al., 2002), as the solubility of CO_2 and the dissociation of carbonic acid in seawater are modulated not only by temperature, but also by changes in ionic strength and instantaneous air-sea exchange (Weiss et al., 1982). The magnitude of DIC_{bio} is mainly related to the uptake or release of DIC attributable to the processes of phytoplankton production and heterotrophic respiration. However the estimate will also incorporate the effects of CO_2 consumption associated with calcite dissolution, a much smaller component of net carbon dynamics in this region, which is related to the biological production rate of calcite (Graziano et al., 2000; Balch et al., 2008).

To calculate DIC_{mix} , we required estimates of riverine and oceanic endmember DIC values. Riverine DIC endmembers were estimated from in-situ pH and TA measurements taken at 0 salinity in the Kennebec (estimated precision $\pm 5.0 \mu\text{mol kg}^{-1}$). Riverine samples were taken within 3 days of each cruise at times corresponding to 11 of the 18 cruises. For the cruise periods when no river samples were taken, we assume a linear interpolation of DIC values between sample dates. This assumption is not expected to introduce significant error at the salinities for which DIC_{bio} and DIC_{mix} are reported (>26), as the average absolute difference in (ca) monthly TA samples at the Kennebec endmember is $37 \mu\text{mol kg}^{-1}$.

Ocean DIC endmember concentrations corresponding to each cruise date were estimated at a location $\sim 65 \text{ km}$ southeast of our most distal station (at $42.8\text{N } -68.2\text{W}$, Fig. 1). For this work, a desirable ocean endmember would exhibit comparatively low biological activity and be located away from the influence of local river mixing. Thus the ocean endmember was selected on the basis of relatively low surface chlorophyll values and weak river influence. The mean satellite derived chlorophyll value (MODIS OC3, 7/2002–6/2006) at this site was $\sim 0.2 \text{ mg m}^{-3}$, which is low compared to the mean of all inshore stations, $\sim 2.4 \text{ mg m}^{-3}$ (<http://www.cooa.unh.edu/data/SR/SR.jsp?tab=collection>). While chlorophyll concentration cannot be considered a measure of biological processes that mediate DIC, it nonetheless is a proxy for living biomass and also weighs strongly in routine satellite productivity models (e.g. Behrenfeld and Falkowski, 1997). Advective tracer studies using the OCM show minimal influence from the coastal plume at this location relative to the inshore stations. DIC at the ocean endmember was estimated with the CO2SYS carbonate

Table 2
Summary of DIC products used in this work.

Product	How produced	Notes
DIC _{observed} (mmol kg ⁻¹)	Estimated from TA and pCO ₂ ; Riverine endmembers estimated from TA and pH	Carbonate system constants from Cai and Wang (1998)
DIC _{mix} (mmol kg ⁻¹)	Conservative mixing of land and ocean DIC endmembers, $f(\text{salinity})$ Wanninkhof (1992) algorithm	Measured river endmember. Estimated ocean endmember
DIC _{air-sea} (mmol kg ⁻¹)		Mass of daily air-sea flux for surface 10 m
DIC _{bio} (mmol kg ⁻¹)	$=\text{DIC}_{\text{conserve}} - (\text{DIC}_{\text{observed}} + \text{DIC}_{\text{air-sea}})$	Stock of DIC mediated by biological processes within surface 10 m

equilibrium equations using modeled SST and salinity at the station location, estimated TA and average regional in-water pCO₂ as inputs. Ocean endmember TA was modeled as a function of salinity using a relationship derived from our entire dataset ($\text{TA} = 56.1(S) + 358$). Mean regional pCO₂ (363 μatm, standard deviation 21.1) is the average of all data from the COOA and Carbon Dioxide Information Analysis Center (CDIAC, <http://cdiac.ornl.gov/>) databases that falls within 0.25 degrees of the distal station ($n = 4893$). The effects of temporal variability of pCO₂ at this site are assumed to be a small fraction of the total DIC budget. For example, the variability imparted to a water parcel from a pCO₂ perturbation of ±21.1 μatm at 34 psu, 20 °C, would be ±9.9 μmol kg⁻¹ DIC. A summary of the DIC products is shown in Table 2. Daily DIC_{bio} values were estimated so that the OCM operating on a daily time step could be used for daily assessments of net DIC_{bio} uptake in the region. Daily DIC_{bio} was estimated by placing a piecewise cubic hermite interpolating polynomial spline (pchip, Matlab™) with a daily time step across the (ca) monthly DIC_{bio} data at each longitudinal interval of 0.01 degrees (Fig. 3b).

In addition to endmember variation discussed above, estimates of DIC_{bio} could be compromised by mixing at time scales different than our sampling interval, or by the introduction of a third (upstream) endmember. For example, if a sampling interval between two successive cruises is considerable longer than the water residence time, initial conditions from which results of the second survey develop may not be properly characterized during the first cruise. Because our region is influenced by advection attributable to the MCC, we used the OCM with a Lagrangian particle-tracking module to estimate the median time for surface waters to flow through the study domain. Since the estimated median lifetime of ~26 days is close to our sampling frequency, we assume that errors arising as a result of ignoring advective losses and gains in the calculation of DIC_{bio} will not significantly alter our results or conclusions. We also assume that water entering from the northeast will be influenced by endmembers that are similar to those in our region. Although this assumption has not been thoroughly tested, we note that the mean TA value for a large river northeast of our region (Penobscot, 301 μmol kg⁻¹, $n = 12$) is similar to the Kennebec.

2.1. Distribution of DIC: the impact of dilution

Temporal variability of salinity and DIC along our cruise track (Fig. 4) suggests the importance of freshwater input as a mechanism driving the variability (see composite hydrograph on Fig. 4, left). Both salinity and DIC followed a seasonal pattern of lower values when discharge was higher. These effects tend to be stronger nearer to the coast. Likewise, the highest salinity and DIC were observed during the late summer when discharge was low, and

during the winter when freezing temperatures typically confine discharge to base flow. In addition to simple dilution, freshwater can induce a shift in the carbonate system equilibrium via heating or cooling, and also through the mixing of low-alkalinity river water with higher-alkalinity ocean water. Thus the variability in carbonate parameters across the salinity gradient is based both on the mixing of DIC endmembers and variability attributable to changes in SST.

The image in Fig. 5a shows a seasonal pattern of riverine influence with the largest DIC depletion occurring during the spring freshet and persisting into the beginning of the summer, presumably consistent with advective time scales of river discharge to the region (Geyer et al., 2004). The most noteworthy feature is the large DIC depletion occurring during ~March–July of 2005 when integrated discharge of the Saco, Kennebec and Merrimack Rivers was highest over a 25-year record. During this depleted DIC period, the region of freshwater influence and the corresponding depression in DIC_{mix} extended throughout the measured domain. The broad pattern of higher DIC_{mix} during the later summer through winter 2004 can be explained by the lower discharge. However, during 2005, the discharge that occurred in October and November was also among the highest for that time period in the USGS 25-year record, at a time when the depletion of DIC was more modest. The frequency of cruises was lowest between October and December of 2005, as a cruise scheduled for November had to be cancelled due to bad weather. As such, we have less confidence in the interpolated values during this period. Nevertheless, the circulation model shows that this was a time in which copious amounts of allochthonous freshwater lowered the salinity in the entire Gulf of Maine. This suggests that the ocean endmember used to calculate DIC_{mix} would have already been diluted by sources of freshwater well upstream of our observation site. Thus the relative contribution of mixing from local sources may have been more difficult to detect using the methods presented above.

2.2. The influence of biology

In addition to mixing, a host of biological processes mediate DIC. These include primary productivity, aerobic and anaerobic respiration, and the precipitation of calcite during shell formation. We assume that in a biologically inert ocean, the primary control of DIC would be from mixing and heat exchange, and that surface water pCO₂ would be close to equilibration with the atmosphere over (ca) monthly time scales. Biological activity represents a perturbation to this mixing field, which is captured as DIC_{bio}. It is estimated as the difference between DIC_{observed} and that inferred from a mixing of oceanic and terrestrial endmembers for which air-sea exchange of DIC has been removed (Fig. 3, Table 2). We assume negative DIC_{bio} values to be the result of biological uptake, primarily from net phytoplankton production, while positive values are the result of net microbial respiration (Raymond et al., 2000; Wang et al., 2005; Schiettecatte et al., 2006).

The generalized pattern of DIC_{bio} (Fig. 5b) follows the seasonality of productivity and respiration in the Gulf of Maine with highs and lows presumably corresponding to the availability of light, nutrients and labile carbon. Productivity-related uptake in the DIC_{bio} field was observed during the spring and early summer of both years and corresponds roughly to the spring blooming of Gulf of Maine waters. The main difference between years is the strong uptake of DIC_{bio} initiated during late winter–early spring of 2005 that persisted into early summer and coincided with the anomalous river discharge phenomena. The weak uptake observed offshore during late summer–fall was likely stimulated by nutrient delivery via upwelling events, as suggested by the offshore movement of the surface fields in the circulation model. Higher offshore

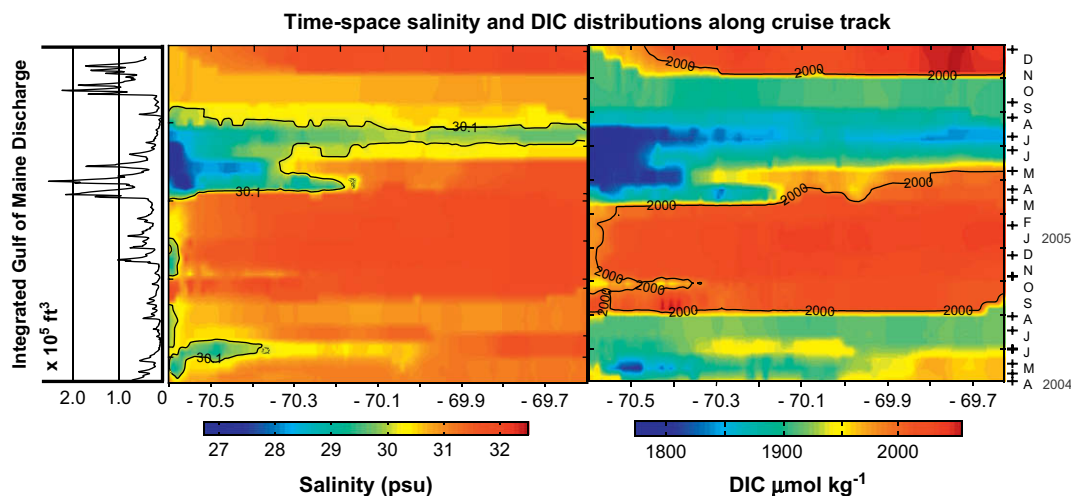


Fig. 4. Discharge, plume area interpolated time–space salinity and DIC fields. Daily USGS discharge gauge data (left) summed for the largest rivers affecting the area of interest (Merrimack, Saco, Kennebec and Penobscot). Cruise transect salinity and DIC data were interpolated in Matlab™ using EasyKrig, written by Dezhong Chu. Anomalously high discharge during the Spring–Summer of 2005 was observed to correspond to depressions both the salinity and DIC fields. Approximate cruise dates are shown as black crosses at the right of the figure.

DIC_{bio} values were observed from late summer into winter. By late summer, the subsidy of limiting nutrient is usually depleted and respiration of previously fixed organic matter dominates the status of community metabolism (Townsend, 1991). Heterotrophy will also dominate through late fall and winter as the availability of light severely limits autotrophic activity. During times of adequate incident light in which DIC_{bio} was positive (Spring Fall), a cross-shore gradient in DIC_{bio} was observed (Fig. 5b). This phenomenon was believed to be the result of respiration of organic matter of terrestrial or near-coastal origin dominating over autotrophic production (e.g. Salisbury et al., 2008).

Biological processes will perturb the DIC field as to increase the difference (delta) between the air and in-water pCO₂ values, facilitating the exchange of CO₂ between the air and sea. The mapped air-sea flux is shown in Fig. 5c. Note that this has been calculated over the entire water column, whereas when estimating DIC_{air-sea}, we account only for the fraction of the air-sea exchange within the 10 m lens of interest (Fig. 3a). The pattern of air-sea CO₂ flux roughly follows the pattern of DIC_{bio} indicating that biology is an important factor in modulating delta pCO₂. However since CO₂ flux is also a function of wind speed (Equation (1)), notable departures from this pattern are seen during periods of higher wind speeds (e.g. October–December, 2005).

2.3. Differences in DIC_{bio} between plume and non-plume waters

The proximity of the region to substantial riverine influx offers an opportunity to examine the effect of riverine influence on the behavior of DIC_{bio}. To segregate our region into plume-influenced and non-plume waters, we arbitrarily chose the plume threshold as a parcel of surface water 10 m in depth having a freshwater equivalent column (H_{FW}) of greater than or equal to 5 cm (see Fig. 2). Non-plume areas were defined as waters adjacent to the plume within the region of interest, with an equivalent freshwater height of less than 5 cm over the surface 10 m. To compare DIC_{bio} behavior within each region, equal volumes of plume and non-plume water were analyzed based on the modeled area of the plume. For this work the upper limit of the Geyer et al. (2004) mean plume thickness (10 m) was chosen as the depth of integration and we assume this lens to be homogeneously mixed in terms of salinity, temperature and the various surface DIC

estimates. Homogeneity of the cruise-averaged DIC_{bio} was also assumed throughout the individual plume and non-plume volumes. In other words, the average values estimated within each region along the cruise track were treated as indicative of the average throughout the spatial extent for each of the plume and non-plume regions.

For each cruise date, average surface DIC_{bio} was calculated for plume and non-plume regions based on the plume threshold. To determine whether the data fell into the plume or non-plume region, all DIC_{bio} data subtended by modeled H_{FW} freshwater anomaly (5-cm freshwater in 10-m) along the cruise track were compiled. These data were averaged and a single DIC_{bio} value was assigned to the entire 10 m plume column. All other DIC_{bio} data were averaged and assigned to the non-plume region. Daily average DIC_{bio} values were estimated by interpolation of the (ca) monthly cruise data (Fig. 6a). These in turn were multiplied by concurrent plume volume calculated from the circulation model ($plume\ area \times 10\ m$) to produce daily 10 m-integrated DIC_{bio} within each region (Fig. 6b). Daily-interpolated DIC values capture the variability provided by the daily-modeled plume volume estimate.

Although it is not possible to completely assess the errors involved in using interpolated daily estimates based on monthly data, an examination of a daily time series of in-water pCO₂ from the PMEL-UNH Coastal Observatory's CO₂ buoy within the study region provides insight (http://www.pmel.noaa.gov/co2/coastal/NH/data_070w_14d.htm). A simple simulation using 186 days of buoy data was run in order to estimate the range of errors that could be attributed to sampling the daily pCO₂ data at increasing time intervals. We found a nearly linear relationship between the time interval of sampling (2–32 days) and the error between an estimate based on interpolation and the average daily measured value. For an average 32-day time interval between repeat cruises, the average absolute error of a daily value (interpolated estimate versus observed) was 5.4%, standard deviation = 21.2 μatm (data range 278–519 μatm). For our DIC_{bio} estimate, we assume that percentage errors in DIC_{bio} are similar to those of pCO₂ since both are modulated by biological processes and were highly correlated ($r^2 = 0.89$) in the dataset used for this paper. While the daily DIC_{bio} estimate can be considered a reasonable proxy for regional DIC_{bio} status, it must be bound by these temporal interpolation errors (see Fig. 6b and c).

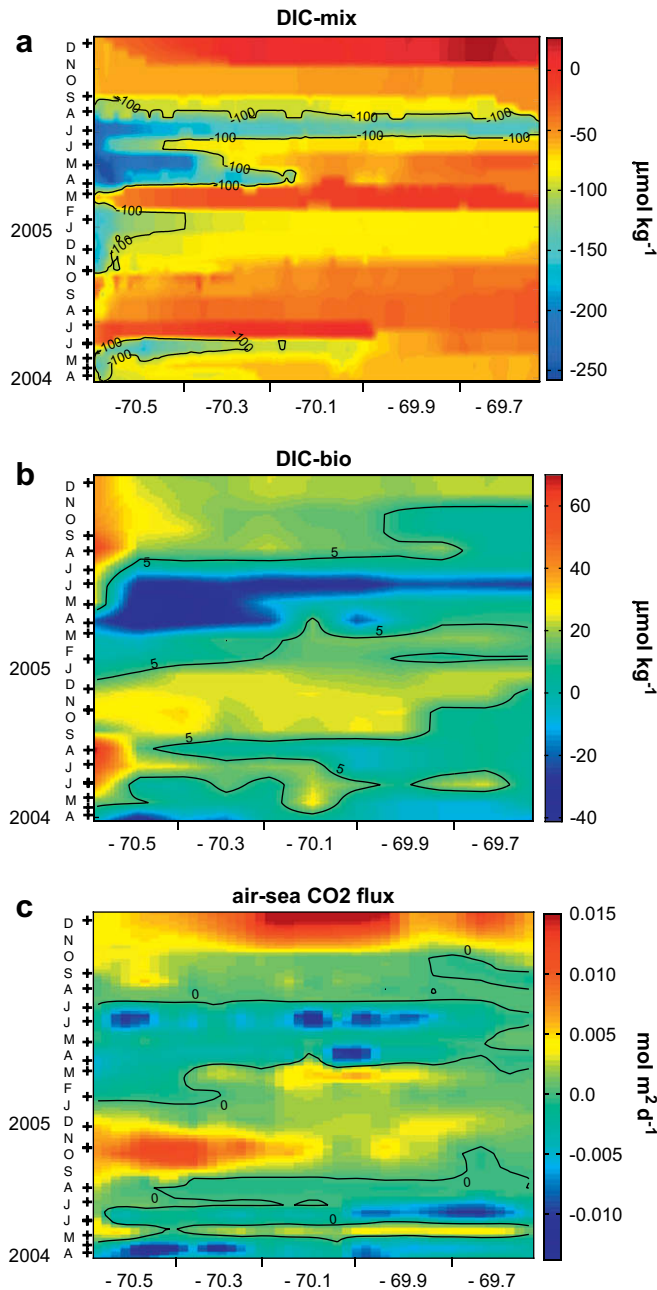


Fig. 5. Interpolated time-space plots from COOA cruise track. Time range (4/19/04–12/17/05); cruise track from approximately: 43.1N, –70.7W, to 42.8N, –69.8W, a distance of ~81 km. (a) DIC_{mix} , (b) DIC_{bio} , (c) air-sea CO_2 flux (see text for methods). Approximate cruise dates are shown as black crosses at the left of the figure.

Differences in the temporal evolution of DIC_{bio} between the plume and non-plume regions are apparent (Fig. 6a). The plume region was more variable with higher average values during the summer through winter of 2004 and a notable decline in values (absent in the non-plume region) during the spring of 2005. Both regions exhibited a dramatic drop in DIC_{bio} values during the extensive discharge events of late spring–early summer 2005. Other than this period, however, the non-plume region had a much smaller range of average values (-19.4 to $12.7 \mu\text{mol kg}^{-1}$) and standard deviation (8.4) compared to the plume region (range -34.4 to $36.1 \mu\text{mol kg}^{-1}$, standard deviation = 13.7). When multiplied by daily plume volume model estimates, the integrated daily

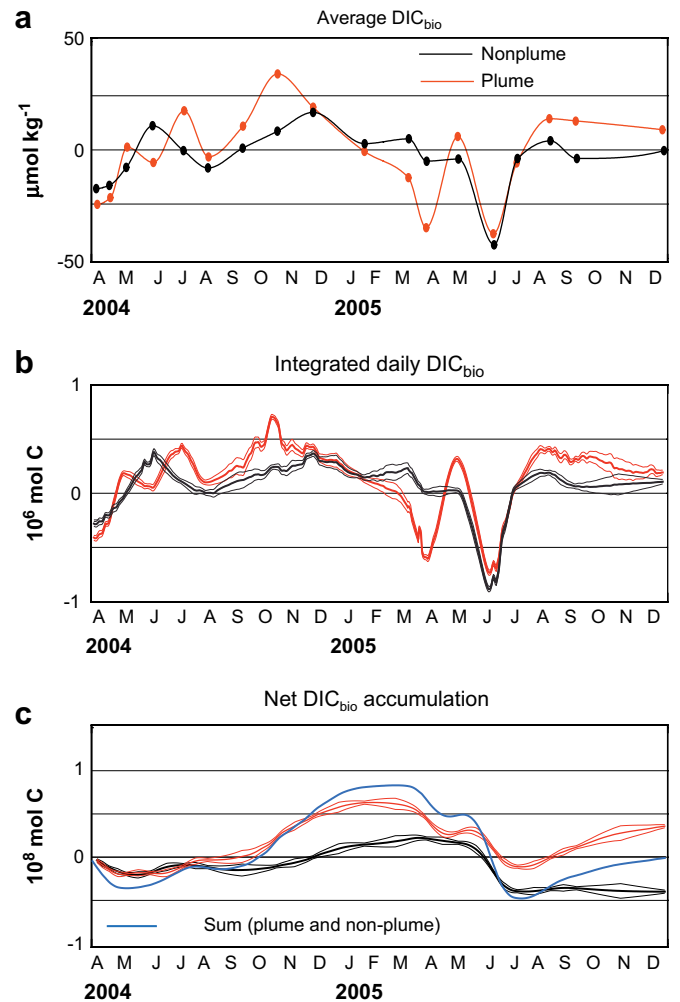


Fig. 6. DIC_{bio} estimations for equal plume and non-plume volumes. Plume and non-plume volumes were set as equal by plume area (i.e. freshwater anomaly >5 cm per 10 m depth \times 10 m plume depth). Density estimates necessary for converting mass of seawater to volume ($v = 1/\rho$) are derived from Millero and Possion (1981), using in-situ SST and surface salinity data. (a) Average DIC_{bio} for plume and non-plume regions of the area of interest. (b) Integrated DIC_{bio} within equal plume and non-plume volumes. These data were estimated as plume volume (daily area estimate (m^2) \times 10 m) \times average DIC_{bio} (mmol m^{-3}). (c) Cumulative curve of daily-integrated DIC_{bio} for equal plume and non-plume volumes. The blue curve is the sum of DIC_{bio} for plume and non-plume curves. Error bounds (in Fig. 6b and c) are a function of the time interval between cruises and are based on the assumption that sampling errors within the DIC_{bio} field would be similar to pCO_2 measured at the PMEL-UNH buoy (see text). (For interpretation of the references to color in this figure legend, the reader is referred to the web version of this article.)

stock of DIC_{bio} for equal plume and non-plume volumes (Fig. 6b) resembled the average DIC_{bio} curves (Fig. 6a). However, the variability imparted by using the daily model plume volumes is obvious and shows the effect of changes in the plume extent on the estimated stock of DIC_{bio} .

Comparative net accumulation plots (Fig. 6c) made from continuous summing of the daily DIC_{bio} values (Fig. 6b) also show differences between the plume and non-plume regions. Both curves start as sinks for DIC_{bio} but by late fall of 2004 the cumulative distribution curves have separated due to high DIC_{bio} accumulation in the plume region. The intense productivity events of 2005 (period of DIC_{bio} uptake) drive both regions into net sinks, with the non-plume region becoming a slightly stronger sink. This shift, which occurs over a time period of less than 3 months,

demonstrates the dramatic effect that a single annual productivity cycle can have on the net annual carbon dynamics of a region. At the end of the observation period (~ 20 months) the plume region was a modest source of DIC_{bio} (3.7×10^7 mol C) while the non-plume province was a modest sink (-4.1×10^7 mol C). Interestingly, for the entire time series the region was apparently balanced in terms of DIC_{bio} , and thus was neither a significant source nor sink (blue curve).

2.4. Comparative DIC_{bio} budgets during the spring freshets of 2004 and 2005

The major anomaly features in Figs. 3 and 4 are associated in time with the high discharge periods of April–June 2005, and allude to the importance of terrestrial freshwater fluxes in the control of DIC and DIC_{bio} . Here we focus on two seasonal periods April 20–June 19 of 2004 and 2005. The cruise time series started in April of 2004 and thus we do not have information on the time of the initiation of the 2004 DIC_{bio} drawdown. Nevertheless, the chosen time intervals were very different in terms of local freshwater flux and associated DIC_{bio} dynamics within the region. Fig. 2, showing the average freshwater heights over these periods, demonstrates this point and suggests the considerable differences in the local freshwater stocks. The figure shows that both the circulation model-estimated extent and volume of the plume-affected region were substantially greater during the 2005 period. Calculations based on the circulation model (Table 3) indicate that the volume of freshwater in 2005 exceeded 2004 by a factor of ~ 6 and that the average areal extent of the plume was 34% larger during 2005. The behavior of DIC_{bio} between the two periods (for the entire region) also showed major differences in terms of averages and net cumulative values (Table 3). The surface lens was estimated to have an average DIC_{bio} value that was much lower during the anomalous discharge period of 2005 than it had during the same period of 2004. Although a biological drawdown of DIC was observed during both periods, 2005 was a stronger sink for DIC_{bio} , with the 2004 period sequestering only $\sim 1/3$ as much carbon as the 2005 period.

3. Discussion

These observations point to conditions where local freshwater inputs contributed to the cycling of DIC both in terms of mixing and biological processing. Although the effects of mixing are obvious, logical questions arise concerning the specific processes related to the presence of freshwater that would impart such variability to the DIC_{bio} fields. Rivers are sources of labile carbon, which will drive heterotrophic respiration, and discharged nutrients that will stimulate autotrophic production. In regions proximal to discharge, higher concentrations of particulate and colored dissolved matter scatter and absorb light, minimizing its availability to phytoplankton thus reducing autotrophic production (Trefry et al., 1994; Cloern, 1996; Lohrenz et al., 1999). Abundant reduced carbon in dissolved and particulate phases can lead to intense heterotrophic respiration (e.g. Zhai et al., 2005). The declining cross-shore gradients with highest DIC_{bio} values proximal to the coast (Fig. 3)

are suggestive of these conditions. Indeed, for the entire time series the plume region was an overall net source of DIC_{bio} , in spite of its much higher sink terms during the productive seasons. This is not unexpected as prevailing arguments lead to the concept that shelf regions strongly influenced by terrestrial fluxes are likely to be net heterotrophic, as labile terrestrial carbon along with a fraction of autotrophic production, is respired (Smith and Hollibaugh, 1993; Cai and Wang, 1998; Zhai et al., 2005; Borges et al., 2008). Conversely, phytoplankton productivity tends to be greatest at the distal reaches of plumes where nutrients may still be adequate, but light penetration depth increases after particle settling has occurred (Cloern, 1996; Smith and Demaster, 1996; Lohrenz et al., 1999). Assuming that these conditions existed in regions directly adjacent to the more turbid plume, they likely contributed to the sustained DIC_{bio} uptake during spring–summer periods.

Variation in pCO_2 within the Kennebec and Merrimack estuaries and adjoining plumes was studied by Salisbury et al. (2008). Although variation was highest in the Merrimack estuary–plume system, both systems changed seasonally between inferred net autotrophic and heterotrophic conditions. The authors concluded that watershed attributes, namely fluxes of labile carbon and nutrients, were responsible for shifts in trophic status within the estuaries and near shore plumes. Since the region of study receives direct input from these systems, and the timing of maximum DIC_{bio} uptake corresponded to the freshet discharge, we were curious if the watershed nutrient fluxes could be an important driver of the spring DIC_{bio} depletions. To test this idea we calculated the flux of the presumed limiting nutrient, dissolved inorganic nitrogen (DIN), to our study region from the Kennebec and Merrimack rivers over the productive periods of April 19–June 18, 2004 and 2005. The calculation was made as the product of integrated discharge (USGS) and DIN concentrations ($\text{m}^3 \times \text{mol m}^{-3}$), using the mean of recent DIN determinations for the Merrimack (2004 data, USGS) and Kennebec (Hunt et al., 2005). These estimates show that if the entire DIN flux of these rivers was processed into biomass within our study area (using a C:N ratio of 6.6:1 (Redfield, 1958)), then $\sim 6.8 \times 10^8$ mol C was produced in 2004 compared to 12.7×10^8 mol C during the same period in 2005. Scaled to annual production throughout the plume region, this amounts to only $1.32 \text{ gC m}^{-2} \text{ y}^{-1}$ for 2004 and $2.42 \text{ gC m}^{-2} \text{ y}^{-1}$ for 2005. While these estimates represent a very small fraction of the annual net primary productivity (NPP) measured in the Gulf of Maine, $250\text{--}400 \text{ gC m}^{-2} \text{ y}^{-1}$ (O'Reilly and Busch, 1984; O'Reilly et al., 1987; Townsend, 1998), it is interesting to note that the carbon sequestered by river DIN is of the same magnitude as the annual estimate of DIC_{bio} within the surface 10 m lens (Table 3). Although this may imply that the riverine DIN could support the net production available for export, this notion is inconsistent with the prevailing model of productivity in the Gulf of Maine that suggests that deep mixing during winter provides the bulk of the nutrients required to fuel seasonal productivity (Townsend, 1992, 1998; Townsend et al., 1994).

The differences in springtime depletion of DIC between the plume and non-plume regions (notably during 2005, Fig. 6a and b) must be a function of availability of light and inorganic nutrients, of which DIN is likely limiting (Townsend, 1998). The ubiquitous tidal mixing of shallow waters in the Western Gulf of Maine is one likely source of DIN that may have a greater influence on the shallower plume waters (e.g. Townsend, 1991; Rogachev et al., 2001). We surmise that storm-driven mixing is also a source of nutrients, although data to support this are sparse in the western Gulf of Maine. However, logic dictates that shallow coastal mixing processes that increase resuspension of particulate matter would also reduce light availability, suppressing autotrophic productivity and subsequent net DIC uptake (e.g. Cloern, 1996). Strong land–ocean gradients in atmospheric DIN deposition (Alexander et al.,

Table 3
Comparison of conditions during April 19–June 18 (2004 and 2005).

Estimate	2004	2005
Average plume (H_{FW}) area (km^2)	17 630	23 596
Average freshwater volume (km^3)	6.8	39.5
Average DIC_{bio} depletion (mmol kg^{-1})	-1.27	-13.97
Net DIC_{bio} accumulation (mol) in region of interest (plume and non-plume)	-0.48E8	-1.33E8

2001) or remineralization of terrestrial organic nitrogen (Mayer et al., 1998) could explain an unknown portion of the difference observed. Periodic coastal upwelling also provides nutrients to the euphotic zone (Townsend, 1991). It has been hypothesized that this region of the Gulf is a “trap” for regenerated nutrients (Townsend and Christensen, 1992). The expression of this trap can be found in numerous observations of anomalous low salinity-high nitrate water, with the highest number of such observations found in the southwestern Gulf. Mixing of the spring freshet with Maine Intermediate Water, which has a characteristic NO_3 concentration of $14.5 \mu\text{mol}$, is thought to be responsible for much of the anomalous salinity-nitrate values observed near the coast (Garside et al., 1996). However we assume processes contributing to such values would influence both domains. Indeed such anomalously low salinity-high nitrate values appear to be widely distributed throughout our entire region of interest (Garside et al., 1996, Fig. 4).

A potential explanation for the differences in biological DIC uptake between the regions invokes the role of riverine discharge as a source of buoyant stability. While speculative, it is possible that the influence of river freshwater could suppress mixing during times of high nutrient concentration, hastening the onset of autotrophic production even during less than optimal light conditions. Higher surface nutrient concentrations and discharge both occur in the early spring, the coincidence of which may provide an opportunity for earlier and more persistent productivity in the plume region versus the non-plume region. Possible mechanisms for phytoplankton blooming in the Gulf of Maine in the absence of stratification were discussed in Townsend et al. (1992). Later, Durbin et al. (2003) reported that freshwater from the Scotian Shelf helped to promote water column stability, which in turn aided the onset of an anomalous (pre-spring) bloom in the central Gulf of Maine during February of 1999. We note that the sustained biological DIC uptake event of 2005 actually began in early March at a time when mean cruise SST was less than 3°C (SST data not shown). It has been suggested that lower temperatures can actually enhance the net productivity in the Gulf of Maine by suppressing microbial and grazing pressures (Townsend et al., 1994). During this time, biological DIC uptake was highest within 25 km of the coast and clearly associated with the river plume (Fig. 5).

Regardless of the nutrient sources and coupled riverine processes fueling productivity, it is clear that community respiration related to consumption of autotrophic production and/or labile terrestrial organic subsidies must be an important control on overall carbon metabolism throughout the region. This notion is supported through the spatio-temporal distribution of positive DIC_{bio} values, and also by contrasting high Gulf of Maine NPP rates (O'Reilly et al., 1987; Townsend, 1998), with the much lower net biological DIC uptake rates reported here. Although a direct comparison of NPP and net biological DIC uptake (i.e. NPP – community respiration) rates are not possible, it follows that if NPP is high and the rate of net biological DIC uptake is low, then community respiration must also be high. For illustration, we contrast reported NPP rates with our biological DIC uptake rate for the 4-month April–July period of 2005. We note that our values are estimated over the surface 10 m only, whereas NPP rates are typically integrated to the 1% light level. Here we assume a Gulf-wide euphotic depth of 50 m, and scale the DIC_{bio} values to 50 m for comparison. Four months (i.e. 1/3) of the annual productivity reported by O'Reilly et al. (1987) would yield 83.3 gC m^{-2} versus our net biological DIC uptake of 22.4 gC m^{-2} . Thus even during the most productive period of our study, it appears that much autotrophic production is rapidly lost, assuming the NPP value used is realistic. The actual difference is related to particulate organic matter consumed by the heterotrophic community combined with losses attributable to sinking, and also to unknown errors inherent in the

two productivity determinations. Assuming the errors were reasonable, it would imply that a large fraction of autotrophic production is lost over short time scales, with little available for export as POC.

While the mechanisms driving DIC_{bio} variability are not fully explained, considerable differences in its temporal distributions between seasons and regions were observed. Questions arise about how DIC_{bio} variability would be affected if the timing and magnitude of local freshwater fluxes were to shift as the result of climate-induced changes in temperature and precipitation. Such changes have recently been reported in New England and the Canadian Maritimes (Hodgkins et al., 2003). Over a 90-year time series of several rivers, the onset of the main freshet is now occurring 4.4–8.6 days earlier, and on average, more of the annual discharge is delivered in March with less in May. Presently the timing of the subsidy of buoyancy, terrestrial carbon, and nutrients delivered through the spring freshet follows on the heels of the spring bloom in the Gulf of Maine, perhaps allowing periods of autotrophic and/or heterotrophic activity to persist beyond the initial spring bloom. A high percentage (~50–60%) of annual riverine nutrient flux (Hunt et al., 2005; Oczkowski et al., 2006), and presumably much of the carbon flux, occurs during the ~2–3 month period of snowmelt. The nature of changes imparted onto coastal ecosystems by changes in the discharge regime as well as anthropogenic forcing (e.g. land use, nutrient enhancement) is an open question. Work on these subjects are limited and we must first seek a better understanding of the connection between coastal productivity and the timing and nature of land-sea fluxes, before we can predict the effects of climate perturbations on riverine influenced coastal ecosystems.

Finally, because of such high variability in the estimates of DIC_{bio} , characterization of an ecosystem in terms of carbon dynamics cannot be done using extrapolations based on short time series. If we assume that 2004 was a year in which DIC behavior was closer to a long-term mean, the anomaly of 2005 highlights possible issues that can arise when tallying coastal carbon budgets based on a limited set of observations. We urge caution when interpreting such budgets. Longer time series of relevant measurements in coastal regions are needed to understand the dynamics of land–ocean interaction, as are buoy arrays that would provide data for coastal carbon budget closure.

4. Conclusions

Our study highlights differences in the temporal dynamics of DIC in plume and adjacent non-plume regions over a 20-month time series. In both regions, conservative mixing of river and saline ocean endmembers had the greatest seasonal influence on surface DIC distributions. However, biological processes were important in both regions especially during the spring and summer of both years. Within the plume region the average biological DIC uptake was much larger ($-14.0 \mu\text{mol l kg}^{-1}$) during the anomalous discharge period of April 19–June 18, 2005 compared to the same period for 2004 ($-1.3 \mu\text{mol l kg}^{-1}$). Integrated over the 10-m surface layer of the study region, biological DIC uptake was ($0.5 \times 10^8 \text{ mol C}$) during April–July of 2004 compared to ($1.3 \times 10^8 \text{ mol C}$) during April–July of 2005. Integrating throughout the 20-month observation period, the plume region was a modest source of DIC ($3.7 \times 10^7 \text{ mol C}$) while the non-plume region was a modest sink ($-4.1 \times 10^7 \text{ mol C}$). Within the dataset, it was difficult to resolve processes responsible for the differences observed in the two regions. However, we suggest that this is due in part to the combined effects of nutrient and labile organic subsidies from the rivers, coupled to the additional buoyant stability provided through freshwater fluxes. Since we observed DIC dynamics that were considerably different in

2004 and 2005, we recommend caution when interpreting coastal carbon budgets based on short time series of observations.

Acknowledgements

We gratefully acknowledge our funding support: NASA NNNH05ZDA001N-NIP, NNNH07ZDA001N-Carbon and NOAA-NA16OC2740. We deeply appreciate the professional efforts of Stanley Glidden, Mike Novak, Shawn Shellito, Christopher Manning, Captain Paul Pelletier and the crew of the RV Gulf Challenger.

References

- Alexander, R.B., Smith, R.A., Schwarz, G.E., Preston, S.D., Brakebill, J.W., Srinivasan, R., Pacheco, P., 2001. Atmospheric nitrogen flux from the watershed of major estuaries of the United States: an application of the SPARROW watershed model. In: Valigura, R.A., Alexander, R.B., Castro, M.S., Meyers, T.P., Paerl, H.W., Stacey, P.E., Turner, R.E. (Eds.), *Nitrogen Loading in Coastal Water Bodies: An Atmospheric Perspective*. Coastal and Estuarine Studies. American Geophysical Union, Washington, DC, pp. 119–170.
- Avery, G.B., Kieber, R., Willey, J., Shank, G., Whitehead, R., 2004. Impact of hurricanes on the flux of rainwater and Cape Fear River water dissolved organic carbon to Long Bay, southeastern United States. *Global Biogeochemical Cycles* 18, doi:10.1029/2004GB002229.
- Balch, W.M., Drapeau, D.T., Bowler, B.C., Booth, E.S., Windecker, L.A., Ashe, A., 2008. Space–time variability of carbon standing stocks and fixation rates in the Gulf of Maine, along the GNATS Transect between Portland, ME, USA and Yarmouth, Nova Scotia, Canada. *Journal of Plankton Research* 30, 119–139.
- Bates, N.R., Knap, A., Michaels, A.F., 1998. The effect of hurricanes on the local to global air-sea exchange of CO₂. *Nature* 395, 58–61.
- Behrenfeld, M.J., Falkowski, P.G., 1997. A consumer's guide to phytoplankton primary productivity models. *Limnology and Oceanography* 42, 1479–1491.
- Borges, A.V., Frankignoulle, M., 2002. Distribution and air-water exchange of carbon dioxide in the Scheldt plume off the Belgian coast. *Biogeochemistry* 59, 41–67.
- Borges, A.V., 2005. Do we have enough pieces of the jigsaw to integrate CO₂ fluxes in the Coastal Ocean? *Estuaries* 28, 3–27.
- Borges, A.V., Delille, B., Frankignoulle, M., 2005. Budgeting sinks and sources of CO₂ in the coastal ocean: diversity of ecosystems counts. *Geophysical Research Letters* 32, L14601, doi:10.1029/2005GL023053.
- Borges, A.V., Ruddick, K., Schiettecatte, L.-S., Delille, B., 2008. Net ecosystem production and carbon dioxide fluxes in the Scheldt Estuarine Plume. *BMC Ecology* 8, 15, doi:10.1186/1472-6785-8-15.
- Cai, W.-J., Dai, M., Wang, Y., 2006. Air-sea exchange of carbon dioxide in ocean margins: a province based synthesis. *Geophysical Research Letters* 33, L12603, doi:10.1029/2006GL026219.
- Cai, W.J., 2003. Riverine inorganic carbon flux and rate of biological uptake in the Mississippi River Plume. *Geophysical Research Letters* 30, 1032, doi:10.1029/2002/GL016312.
- Cai, W.-J., Wang, Y., 1998. The chemistry, fluxes and sources of carbon dioxide in the estuarine waters of the Satilla and Altamaha Rivers, Georgia. *Limnology and Oceanography* 43, 657–668.
- Cloern, J.E., 1996. Phytoplankton bloom dynamics in coastal ecosystems: a review with some general lessons from sustained investigation of San Francisco Bay, California. *Reviews of Geophysics* 34, 127–168.
- Depetris, P.J., Kemp, S., 1993. Carbon dynamics and sources in the Parana River. *Limnology and Oceanography* 38, 382–395.
- Dickson, A., 2001. Reference materials for oceanic measurements. *Oceanography* 14, 21–22.
- DOE, 1994. Handbook of methods for the analysis of the various parameters of the carbon dioxide system in seawater (version 2). In: Dickson, A.G., Goyet, C. (Eds.), ORNL/CDIAC-74.
- Durbin, E., Campbell, R., Casas, M., Ohman, M., Niehoff, B., Runge, J., Wagner, M., 2003. Interannual variation in phytoplankton blooms and zooplankton productivity and abundance in the Gulf of Maine during winter. *Marine Ecology Progress Series* 254, 81–100.
- Fong, D.A., Geyer, W.R., Signell, R.P., 1997. The wind-forced response of a buoyant coastal current: observations of the western Gulf of Maine plume. *Journal of Marine Systems* 12, 69–81.
- Fong, D.A., Geyer, W.R., 2002. The alongshore transport of freshwater in a surface-trapped river plume. *Journal of Physical Oceanography* 32, 957–972.
- Frankignoulle, M., Abril, G., Borges, A., Bourge, I., Canon, C., Delille, B., Liebert, E., Theate, J.M., 1998. Carbon dioxide emission from European estuaries. *Science* 282, 434–436.
- Fujii, M., Yamanaka, Y., 2008. Effects of storms on primary productivity and air-sea CO₂ exchange in the subarctic western North Pacific: a modeling study. *Biogeosciences* 5, 1189–1197.
- Garside, C., Garside, J.C., Keller, M.D., Sieracki, M.E., 1996. The formation of high nutrient-low salinity waters in the Gulf of Maine: a nutrient trap? *Estuarine, Coastal and Shelf Science* 42, 617–628.
- Geyer, W.R., Signell, R.P., Fong, D.A., Wang, J., Anderson, D.M., Keafer, B.P., 2004. The freshwater transport and dynamics of the western Maine coastal current. *Continental Shelf Research* 24, 1339–1357.
- Graziano, L., Balch, W., Drapeau, W.D., 2000. Organic and inorganic carbon production in the Gulf Of Maine. *Continental Shelf Research* 20, 685–705.
- Hodgkins, G.A., Dudley, R.W., Huntington, T.G., 2003. Changes in the timing of high river flows in New England over the 20th century. *Journal of Hydrology* 278, 244–252.
- Hunt, C.W., Loder, T., Vorosmarty, C., 2005. Spatial and temporal patterns of inorganic nutrient concentrations in the Androscoggin and Kennebec Rivers, Maine. *Water, Air and Soil Pollution* 163, 303–323.
- Kawahata, H., Suzuki, A., Gupta, L.P., Ohta, H., 2001. Decrease in the CO₂ fugacity during a hurricane event. In: 6th International Carbon Dioxide Conference. Tohoku Univ, Sendai, Japan.
- Kortzinger, A., 2003. A significant CO₂ sink in the tropical Atlantic Ocean associated with the Amazon River plume. *Geophysical Research Letters* 30 (2287), doi:10.1029/2003GL018841.
- Lewis, E., Wallace, D.W.R., 1998. Program Developed for CO₂ System ORNL/CDIAC-105. Carbon Dioxide Information Analysis Center, Oak Ridge National Laboratory, U.S. Department of Energy, Oak Ridge, Tennessee.
- Liu, K.-K., Atkinson, L., Chen, C.T.A., Gao, S., Hall, J., Macdonald, R.W., Talaue McManus, L., Quiñones, R., 2000. Exploring continental margin carbon fluxes on a global scale. *EOS. Transactions – American Geophysical Union* 81 (52), 641.
- Lohrenz, S.E., Fahnenstiel, G.L., Redalje, D.G., 1999. Nutrients, irradiance and mixing as factors regulating primary production in coastal waters impacted by the Mississippi plume. *Continental Shelf Research* 19, 1113–1141.
- Mahadevan, A., Campbell, J.W., 2002. Biogeochemical patchiness at the sea surface. *Geophysical Research Letters* 29, 1926, doi:10.1029/2001GL014116.
- Mayer, L.M., Keil, R.G., Macko, S.A., Joye, S.B., Ruttenberg, K.C., Aller, R.C., 1998. The importance of suspended particulates in riverine delivery of bioavailable nitrogen to coastal zones. *Global Biogeochemical Cycles* 12, 573–579.
- Millero, F.J., Graham, T.B., Huang, F., Bustos-Serrano, H., Pierrot, D., 2006. Dissociation constants of carbonic acid in seawater as a function of salinity and temperature. *Marine Chemistry* 100, 80–94.
- Millero, F.J., Possion, A., 1981. International one atmosphere equation of state for seawater. *Deep Sea Research* 28, 625–629.
- Oczkowski, A.J., Pellerin, B.A., Hunt, C.W., Wollheim, W.M., Vorosmarty, C.J., Loder, T.C., 2006. The role of snowmelt and spring rainfall in inorganic nutrient fluxes from a large temperate watershed, the Androscoggin River basin (Maine and New Hampshire). *Biogeochemistry* 80, 191–203.
- O'Reilly, J.E., Busch, D.A., 1984. Phytoplankton primary production on the northwestern Atlantic shelf. *Rapports et Proces-Verbaux des Reunions Conseil Permanent International pour l'Exploration de la Mer* 183, 255–268.
- O'Reilly, J.E., Evans-Zetlin, C., Busch, D.A., 1987. Primary production. In: Backus, R.H. (Ed.), *Georges Bank*. MIT Press, Cambridge, MA, pp. 220–233.
- Padin, X.A., Vazquez-Rodriguez, M., Rios, A.F., Perez, F.F., 2007. Atmospheric CO₂ measurements and error analysis on seasonal air-sea CO₂ fluxes in the Bay of Biscay. *Journal of Marine Systems* 66, 285–296.
- Perrie, W., Zhang, W., Xuejuan, R., Long, Z., Hare, J., 2004. The role of mid-latitude storms on air-sea exchange of CO₂. *Geophysical Research Letters* 31, L09306, doi:10.1029/2003GL019212.
- Petrie, B., 2007. Does the North Atlantic oscillation affect hydrographic properties on the Canadian Atlantic continental shelf? *Atmosphere-Ocean* 45, 141–151.
- Raymond, P.A., Bauer, J.E., Cole, J.J., 2000. Atmospheric CO₂ evasion, dissolved inorganic carbon production, and net heterotrophy in the York River estuary. *Limnology and Oceanography* 45, 1707–1717.
- Redfield, A.C., 1958. The biological control of chemical factors in the environment. *American Scientist* 46, 205–221.
- Robinson, A.R., Brink, K.H. (Eds.), 2005. *The Global Coastal Ocean: Multiscale Interdisciplinary Processes*. The Sea, vol. 13. Harvard University Press, Cambridge, Massachusetts, 1033 pp.
- Rogachev, K.A., Carmack, E.C., Salomatin, A.S., 2001. Lunar fortnightly modulation of tidal mixing near Kashevarov Bank, Sea of Okhotsk, and its impacts on biota and sea ice. *Progress in Oceanography* 49, 373–390.
- Salisbury, J., Vandemark, D., Hunt, C.W., Campbell, J.W., McGillis, W., McDowell, W., 2008. Seasonal observations of surface waters in two Gulf of Maine estuary–plume systems: relationships between watershed attributes, optical measurements and surface pCO₂. *Estuarine Coastal and Shelf Science* 77, 245–252.
- Schiettecatte, L.-S., Gazeau, F., Van der Zee, C., Brion, N., Borges, A.V., 2006. Time series of the partial pressure of carbon dioxide (2001–2004) and preliminary inorganic carbon budget in the Scheldt plume (Belgian coast waters). *Geochemistry, Geophysics, Geosystems* (G3) 7.
- Smith, S.V., Hollibaugh, J.T., 1993. Coastal metabolism and the oceanic organic-carbon balance. *Reviews of Geophysics* 31, 75–89.
- Smith, W.O., Demaster, D.J., 1996. Phytoplankton biomass and productivity in the Amazon River plume: correlation with seasonal river discharge. *Continental Shelf Research* 16, 291–319.
- Takahashi, T., Sutherland, S., Sweeney, C., Poisson, A., Metz, N., Tilbrook, B., Bates, N., Wanninkhof, R., Feely, R., Sabine, C., Olafsson, J., Njirai, Y., 2002. Global sea-air CO₂ flux based on climatological surface ocean pCO₂, and seasonal biological and temperature effects. *Deep-Sea Research Part II Topical Studies in Oceanography* 49, 1601–1622.

- Townsend, D.W., 1998. Sources and cycling of nitrogen in the Gulf of Maine. *Journal of Marine Systems* 16, 283–295.
- Townsend, D.W., Cammen, L.M., Holligan, P.M., Campbell, D.E., Pettigrew, N.R., 1994. Causes and consequences of variability in the timing of spring phytoplankton blooms. *Deep-Sea Research* 41, 747–765.
- Townsend, D.W., Christensen, J.P., 1992. A nutrient trap in the Western Gulf of Maine. In: *Proceedings of the Gulf of Maine Scientific Workshop*. Woods Hole Oceanographic Institute, Woods Hole.
- Townsend, D.W., 1992. An overview of the oceanography and biological productivity of the Gulf of Maine, pp. 5–26. In: Townsend, D.W., Larsen, P.F. (Eds.), *The Gulf of Maine*. NOAA Coastal Ocean Program, Regional Synthesis Series, No. 1, 135 pp.
- Townsend, D.W., 1991. Influences of oceanographic processes on the biological productivity of the Gulf of Maine. *Reviews in Aquatic Sciences* 5, 211–230.
- Trefry, J.H., Eadie, B.J., Metz, S., Nelsen, T.A., Trocine, R.P., 1994. Transport of particulate organic carbon by the Mississippi River and its fate in the Gulf of Mexico. *Estuaries* 17, 839–849.
- Tsunogai, S., Watanabe, S., Sato, T., 1999. Is there a “continental shelf pump” for the absorption of atmospheric CO₂? *Tellus Series B Chemical and Physical Meteorology* 51, 701–712.
- Wang, Z.A., Cai, W., Wang, Y., Ji, H., 2005. The southeastern continental shelf of the United States as an atmospheric CO₂ source and an exporter of inorganic carbon to the ocean. *Continental Shelf Research* 25, 1917–1941.
- Wanninkhof, R., Olsen, A., Triñanes, J., 2007. Air-sea CO₂ fluxes in the Caribbean Sea from 2002–2004. *Journal of Marine Systems* 66, 272–284.
- Wanninkhof, R., 1992. Relationship between wind-speed and gas-exchange over the ocean. *Journal Of Geophysical Research – Oceans* 97, 7373–7382.
- Wanninkhof, R.H., Thoning, K., 1993. Measurement of fugacity of CO₂ in surface water using continuous and discrete sampling methods. *Marine Chemistry* 44 (2–4), 189–204.
- Weiss, R.F., Jahnke, R.A., Keeling, C.D., 1982. Seasonal effects of temperature and salinity on the partial pressure of CO₂ in seawater. *Nature* 300, 511–513.
- Xue, H., Shi, L., Cousins, S., Pettigrew, N.R., 2005. The GoMOOS nowcast/forecast system. *Continental Shelf Research* 25, 2122–2146.
- Yuan, J., Miller, R.L., Powell, R.T., Dagg, M.J., 2004. Storm-induced injection of the Mississippi River plume into the open Gulf of Mexico. *Geophysical Research Letters* 31, L09312, doi:10.1029/2003GL019335.
- Zhai, W., Dai, M., Cai, W.J., Wang, Y., Wang, Z., 2005. High partial pressure of CO₂ and its maintaining mechanism in a subtropical estuary: the Pearl River estuary, China. *Marine Chemistry* 93, 21–32.